Published in final edited form as:
Neuron. 2011 December 22; 72(6): 938–950. doi:10.1016/j.neuron.2011.12.002.

A CRE-DEPENDENT, ANTEROGRADE TRANS-SYNAPTIC VIRAL TRACER FOR MAPPING OUTPUT PATHWAYS OF GENETICALLY MARKED NEURONS

Liching Lo[1,2] and **David J. Anderson**[1,2,3]

[1]Division of Biology 156-29, California Institute of Technology, 1201 E. California Blvd, Pasadena, CA 91125

[2]Howard Hughes Medical Institute, California Institute of Technology, 1201 E. California Blvd, Pasadena, CA 91125

SUMMARY

Neurotropic viruses that conditionally infect or replicate in molecularly defined neuronal subpopulations, and then spread trans-synaptically, are powerful tools for mapping neural pathways. Genetically targetable retrograde trans-synaptic tracer viruses are available to map the inputs to specific neuronal subpopulations, but an analogous tool for mapping synaptic outputs is not yet available. Here we describe a Cre recombinase-dependent, anterograde trans-neuronal tracer, based on the H129 strain of herpes simplex virus (HSV). Application of this virus to transgenic or knock-in mice expressing Cre in peripheral neurons of the olfactory epithelium or the retina reveals widespread, polysynaptic labeling of higher-order neurons in the olfactory and visual systems, respectively. Polysynaptic pathways were also labeled from cerebellar Purkinje cells. In each system, the pattern of labeling was consistent with classical circuit-tracing studies, restricted to neurons and anterograde-specific. These data provide proof-of-principle for a conditional, non-diluting anterograde trans-synaptic tracer for mapping synaptic outputs from genetically marked neuronal subpopulations.

INTRODUCTION

A central objective in deciphering the neural circuitry of the brain is to define the synaptic inputs and outputs of specific neuronal subpopulations in different regions (Bohland *et al*., 2009). These input/output relationships can be comprehensively mapped by serial electron microscope (EM) reconstruction (Jurrus et al., 2009; Kleinfeld et al., 2011; Ward et al., 1975). However such methods are currently best suited to elucidating microcircuitry within relatively small volumes of brain tissue (Bock *et al*., 2011; Briggman *et al*., 2011), rather than to mapping long-range projections (Seung, 2009). The latter can be visualized using neuroanatomical tracers to sample connections between regions (reviewed in (Kobbert *et al*., 2000; Vercelli *et al*., 2000)). Classical tracers, such as biotin-dextran amine (BDA), fluorescent latex microspheres (Katz *et al*., 1984) or phytohemagglutinin lectin (PHAL),

[3]Author for correspondence Tel: (626) 395-6821, FAX: (626) 564-8243 wuwei@caltech.edu.

have provided much useful information (e.g., see (Swanson, 2000)), but they reveal axonal projections, not synaptic connections, and can be difficult to genetically target.

The use of site-specific recombinases (Branda and Dymecki, 2004; Dymecki *et al*., 2010) and other tools for driving heterologous gene expression in mice has allowed the targeting of genetically encoded projection markers, such as GFP, to molecularly defined neuronal subpopulations (Luo *et al*., 2008). These tools also permit genetic targeting of trans-synaptic tracers, which can reveal the synaptic connections of the targeted cells (Callaway, 2008). Plant lectins such as wheat germ agglutinin (WGA) or barley lectin (BL) were among the first genetically targeted trans-synaptic tracers ((Braz et al., 2002; Horowitz et al., 1999; Yoshihara, 2002; Yoshihara et al., 1999); reviewed in (Kobbert *et al*., 2000; Vercelli *et al*., 2000)). Tetanus toxin C-fragment has also been used in this manner (Kissa *et al*., 2002). However WGA is transported in both the retrograde and anterograde direction (Kobbert *et al*., 2000), making the analysis of directionality complex. Furthermore such non-replicating tracers undergo dilution at each synapse, limiting the number of connections that can be detected in a given experiment.

Viruses are especially useful as genetically targeted trans-neuronal tracers, because their replication prevents such dilution, and because they are often transported in a unidirectional manner (for reviews, see (Callaway, 2008; Ekstrand et al., 2008; Song et al., 2005; Ugolini, 2010)). Such viruses include rabies (Astic *et al*., 1993), vesicular stomatitis virus (VSV) (Lundh, 1990), pseudorabies virus (Card and Enquist, 1999; Martin and Dolivo, 1983), Herpes Simplex Viruses 1 and 2 (HSV-1, HSV-2) (Bak *et al*., 1977; Norgren and Lehman, 1998) and Sindbis virus (Ghosh *et al*., 2011). The Bartha strain of pseudorabies virus (PRV; a herpes virus) (Ekstrand *et al*., 2008), as well as rabies virus, travel retrogradely (Ugolini, 2010), while VSV has been modified to travel either in a retrograde or anterograde manner (Beier *et al*., 2011). These viruses have also been targeted to molecularly defined neuronal subtypes using Cre recombinase or an avian receptor, TVA, in transgenic mice (Card et al., 2011a; Card et al., 2011b; DeFalco et al., 2001; Wall et al., 2010; Weible et al., 2010; Wickersham et al., 2007; Yoon et al., 2005). The rabies virus system has been further modified to cross only one synapse (Wall et al., 2010; Weible et al., 2010; Wickersham et al., 2007). Although the relative merits of the rabies and pseudorabies systems continue to be debated (Ekstrand *et al*., 2008; Ugolini, 2010), they have each been profitably used to extract useful information about the connectional organization of specific circuits.

While conditional trans-synaptic tracer viruses are available to map the synaptic inputs to genetically marked neuronal subpopulations (DeFalco et al., 2001; Haubensak et al., 2010; Wall et al., 2010; Weible et al., 2010; Wickersham et al., 2007), an analogous anterograde-specific trans-synaptic viral tracer for mapping synaptic outputs is not yet available. An anterogradely transported, cell-targetable variant of VSV has shown promise in hippocampal slice cultures (Beier *et al*., 2011), but this conditional variant has not yet been tested and validated in vivo. The HSV-1 strain H129 (Dix *et al*., 1983) is an attractive candidate for developing a conditional anterograde trans-neuronal tracer virus (Zemanick *et al*., 1991). In its native form, H129 has been utilized to trace circuitry in the rodent visual (Archin et al., 2003; Sun et al., 1996), viscerosensory (Rinaman and Schwartz, 2004), trigeminal (Barnett *et al*., 1995), and white adipose sensory pathways (Song *et al*., 2009), as well as primary motor cortex (Kelly and Strick, 2003; Zemanick et al., 1991), and spinothalamic (Dum *et al*., 2009) pathways in non-human primates. However, a conditional, Cre-dependent version of H129 that can be used to trace neural circuitry *in vivo* has not previously been reported. Here we develop, characterize and validate such a virus *in vivo*. Our results provide a novel method for mapping the synaptic outputs of genetically marked neuronal subsets.

RESULTS

To develop a conditional H129 strain-based tracer, we simultaneously inactivated the endogenous H129 viral *HTK* gene and replaced its coding sequence with a Cre-dependent *loxP-STOP-loxP-tdTomato-2A-TK* cassette (Fig. 1A) via homologous recombination (Archin et al., 2003; Weir and Dacquel, 1995), using a codon-modified form of *HTK* to prevent recombination within the coding sequence (cmHTK; Supplemental Experimental Procedures). After co-transfection of the HTK targeting vector and native H129 genomic DNA into host cells, H129 recombinants were selected by picking acyclovir-resistant plaques (Fig. 1B; see Experimental Procedures) and validated using PCR (Fig 1C). The resulting H129 recombinant was named H129ΔTK-TT (tdT HTK). Infection of cultured Vero cells with this virus revealed specific expression of tdT only in the presence of Cre (Fig. 1D, E). Recombined virus recovered from such cells and used to infect naive Vero cells rendered the latter sensitive to acyclovir-dependent killing, indicating that the cmHTK was enzymatically active (data not shown).

Cre-dependent, poly-synaptic anterograde labeling of Purkinje cell circuitry

As an initial test of the Cre-dependent H129ΔTK-TT system in vivo, virus was injected intracranially into the medial cerebellar vermis of PCP2/L7-Cre transgenic mice (JAX Stock #006207), which express Cre and GFP specifically in Purkinje cells (Barski et al., 2000; Oberdick et al., 1990; Zhang et al., 2004). Four days following infection, GFP-positive Purkinje cells in PCP2/L7-Cre/GFP mice co-expressed tdT, and all tdT-positive cells were GFP-positive (Fig. 2C). We rarely saw tdT expression in other cell types in the cerebellar cortex, except in regions close to the site of injection exhibiting substantial tissue necrosis, where we observed some labeled granule cells (not shown). However, labeled granule cells were not observed outside of the necrotic zone, arguing against retrograde or non-synaptic transfer of recombined H129ΔTK-TT virus. Wild type mice injected with H129ΔTK-TT showed no tdT expression in virally infected cells (identified by HSV-1 antigen expression; Fig. 2B) as assessed both by native fluorescence and by anti-dsRED antibody staining (data not shown), indicating minimal leakage from the loxP-STOP-loxP cassette (Zinyk *et al*., 1998).

We next examined labeling of cerebellar circuitry downstream of Purkinje cells in these mice. Purkinje cells axons, which are the main efferents from the cerebellar cortex, target the deep cerebellar nuclei (DCN). In H129ΔTK-TT infected mice, tdT could be detected in most of the three major subdivisions of the DCN--the fastigial nuclei (FN), the interposed nuclei (IP), and the dentate nucleus (DN) (Fig. 2D-F). We also detected labeling in known DCN targets (Ito, 1984), including the vestibular nuclei (VE; Fig. 2G-I), the inferior olive (IO; Figure 2J-L), ventral lateral thalamus (VL; Figure 2M-O) and the red nucleus (RN; Supplemental Figure 1M-O). Labeling was also observed in the interpeduncular nuclei, a target of fastigial axons (Snider *et al*., 1976) (Supplemental Figure 1G-I), and in the hippocampus and cortical amygdala (Supplemental Figure 1J-L).

tdT labeling in all these structures was present in cell somata, as determined by counter-staining with fluorescent Nissl (Fig. 1F, I, L, O). We determined the neuronal vs. glial identity of these cells by co-staining with antibody markers. In the inferior olive (IO), the majority of tdT expressing cells co-expressed the pan-neuronal marker NeuN (333/395; 85%), while only a very small percentage (1/45; 2%) co-expressed GFAP (Figure 2P-R and Supplemental Fig. 2A-H). Qualitatively similar results were observed in the area postrema (AP) and nucleus of the solitary tract (NTS), two additional sites where anterograde labeling from infected Purkinje cells was detected (Ross *et al*., 1981), and in the VPL (Supplemental Figure 2I-X and Supplemental Table 1). These data indicate that the majority of tdT expressing cells labeled in the cerebellar pathway by H129ΔTK-TT virus are neurons.

Unexpectedly, we observed tdT labeling in DBH^+ neurons within the locus coeruleus (LC) (Supplemental Figure 1A-C), which are known to project to Purkinje cells (Hoffer *et al*., 1973). Such LC labeling was not reported in previous trans-synaptic labeling studies using wheat germ agglutinin (WGA) expressed from the same PCP/L7 promoter element, either in AAV (Braz *et al*., 2002) or in transgenic mice (Yoshihara, 2002; Yoshihara et al., 1999). This labeling could therefore reflect retrograde transport of recombined virus released from infected Purkinje cells. However we found that tdT-positive LC neurons ectopically expressed the co-integrated L7/PCP2-GFP/Cre transgene (Supplemental Figure 1D-F and data not shown). Thus, tdT expression in LC neurons may reflect direct infection of terminals of Cre-expressing noradrenergic neurons by virus injected into in the Purkinje cell layer (Supplemental Figure 1P-Q). Alternatively, the tdT labeling could reflect poly-synaptic anterograde projections from Purkinje cells to the LC via the DCN and fastigial axons (Snider, 1976).

All together, approximately 5% (43/836) of anatomically defined brain structures (Franklin and Paxinos, 2008) were labeled in cerebellar injected PCP2/L7-Cre mice (Supplemental Table 3a). Structures such as the RN, which lie several synapses away from Purkinje cells, tended to exhibit a smaller percentage of labeled cells than lower-order targets, such as the DCN, at the time points surveyed (Supplemental Fig. 1N,O vs. Fig. 2E, F and Supplemental Figure 5A).

Cre-dependent, Multi-synaptic Labeling of Visual Circuitry Using H129ΔTK-TT

We next examined the detailed pattern of labeling by H129ΔTK-TT in the visual system (Fig. 3A and (Peters, 1985)), which has been mapped previously using native H129 virus (Sun *et al*., 1996). We used the PCP2/L7-Cre transgenic line for this test, since Cre expression in these mice marks rod bipolar cells (RBCs) in the retina (Fig. 3B and (Oberdick et al., 1990; Zhang et al., 2005; Zhang et al., 2004)). At 5-8 days following monocular intravitreal injection of PCP2/L7-Cre mice, we observed tdT expression in the retina (Fig. 3C). Labeling in the inner nuclear layer (INL) was detected in cells expressing protein kinase C-α (PKCα) (Fig. 3D, arrow), a marker of RBCs (Yamashita and Wassle, 1991)). tdT-positive cells co-expressing calretinin (31 tdT^+/52 $calretinin^+$ cells, n=6 sections) were also detected in the INL, and likely represent amacrine cells (Fig. 3E, arrow) (Kolb, 1981), which are direct post-synaptic targets of RBCs (Wassle, 2004). In the ganglion cell layer, tdT expression was detected in retinal ganglion cells (RGCs), marked by expression of PKCα or calretinin (Fig. 3D, E; arrowheads, respectively) (Haverkamp, 2000).

These data are consistent with the fact that RBCs project indirectly to RGCs via amacrine cells (reviewed in (Wassle, 2004)). In contrast, tdT expression was detected neither in the photoreceptor layer, visualized using anti-arrestin antibody (Fig. 3F), nor in horizontal cells (detected using anti-calbindin antibody; Fig. 3G-I, 0 tdT^+/98 $calbindin^+$ cells); the latter receive synaptic input from cone bipolar but not rod bipolar cells (Wassle, 2004). We also observed almost no detectable tdT in the Edinger-Westphal nuclei, which contain midbrain oculomotor neurons that innervate the eye (data not shown). Together, these data support previous studies indicating that the H129 virus is transported in an anterograde specific manner in the visual system (Sun *et al*., 1996), and also argue that non-synaptic spread from "starter" Cre-expressing cells to neighboring neurons (e.g., horizontal cells) does not occur at an appreciable level.

Labeling of central visual pathways with H129ΔTK-TT

In animals analyzed at 5-8 days post injection (DPI), we observed significant tdT expression in the dorsal lateral geniculate nucleus (dLGN; Figure 3J-L, arrow) and ventral lateral geniculate (vLGN; Figure 3J-L, arrowhead). Counterstaining with fluorescence Nissl

confirmed tdT expression in cell bodies (Fig. 3L), suggesting trans-synaptic transport from RGCs. tdT expression was also detected in layer 4 of area 17 of the visual cortex (Figure 3M-O, arrow), which receives input from the dLGN (Frost and Caviness, 1980; Simmons *et al*., 1982). A few tdT positive cells were also found in area 18a, which is located rostrolaterally to area 17 (Figure 3N), indicating transport of the virus across at least 4 synapses from "starter" Cre-expressing RBCs. The lack of detectable tdT expression in layer 5 or 6 of V1, cells of which project to the LGN or SC (Brumberg et al., 2003; Kozloski et al., 2001; Simmons et al., 1982), suggests an absence of retrograde labeling of these cortical neurons, further supporting an anterograde-specific spread of H129ΔTK-TT (Sun *et al*., 1996).

Transport of H129ΔTK-TT to sub-cortical retino-recipient targets

The most abundant direct sub-cortical retinal projection is to the superior colliculus (SC) in the midbrain (Drager, 1974; Provencio *et al*., 1998). In intravitreally injected PCP2/L7-Cre mice, robust tdT expression was seen in the SC at 7 DPI (Figure 3P-R, arrow). tdT labeling was also observed in pretectal nuclei (PT), such as the posterior pretectal nucleus (PPT), the nucleus of the optic tract (NOT) and the olivary pretectal nuclei (OPN), which receive direct input from the retina (Pak *et al*., 1987) (Figure 3K, asterisk; Supplemental Figure 3A-C), as well as in accessory optic tract terminal nuclei such as the medial terminal nucleus (MTN) (Pak *et al*., 1987) (Supplemental Figure 3D-F).

RGCs project to a number of hypothalamic targets, including the suprachiasmatic nucleus (SCN) (Millhouse, 1977) and anterior hypothalamic nucleus (AH) (Hattar *et al*., 2006). We observed abundant tdT expression in both of these structures (Figure 3S-U), as well as in the peri-supraoptic nucleus (pSON) (Hattar *et al*., 2006) (Supplemental Figure 3G-I). tdT-positive cells were also detected in a variety of other hypothalamic nuclei including the PVH (Supplemental Figure 3J-LL and data not shown). Prominent expression of tdT was also seen in the lateral septum ventral (LSV) (Supplemental Figure 3M-O, arrow), a structure which, like the PVH, has been implicated in stress and anxiety (Sheehan *et al*., 2004).

Other structures in which tdT was detected included the medial amygdalar (MEA) and posteromedial cortical amygdalar nuclei (PMCO), and hippocampal layer CA1 (Supplemental Table 3b and data not shown). Overall, approximately 4.4% (37/836) of brain sub-structures (Franklin and Paxinos, 2008) contained tdT label in animals analyzed between 5 and 8 DPI (Supplemental Table 3b). On average, between 5 to 15% of total Nissl positive cells in a 20X field were tdT-positive in each region surveyed (Supplemental Figure 5B). Only 16% (6/37) of the labeled structures in the visual pathway were also labeled in mice traced through the cerebellar pathway using the same PCP2/L7-Cre line (see above), further suggesting that transport is restricted to synaptically connected neurons in specific circuits.

Cre-dependent, poly-synaptic anterograde labeling of olfactory pathways

As a third model system, we tested the H129ΔTK-TT virus in the olfactory system, whose early stages of connectivity are well characterized. The olfactory marker protein (OMP) is selectively and abundantly expressed by mature olfactory and vomeronasal organ (VNO) sensory neurons (Danciger *et al*., 1989). Previous studies using cis-acting elements of OMP to express WGA in these sensory neurons have visualized transport of WGA to second and third order neurons (Horowitz et al., 1999; Yoshihara, 2002; Yoshihara et al., 1999). We therefore examined the pattern of transneuronal labeling following intra-nasal instillation of H129ΔTK-TT virus in OMP-Cre mice (Eggan *et al*., 2004). Among such mice, 27% (7/26) developed various degrees of adverse symptoms a week after injection; the remaining 19 animals never showed symptoms (Supplemental Table 2). Post-mortem analysis indicated

that the severity of symptoms correlated with the efficiency of viral expression; asymptomatic animals typically exhibited little or no infection.

In mildly symptomatic animals (see below), tdTomato could be detected in the main olfactory epithelium (MOE) (Fig. 4B-C). Based on the characteristic cellular morphology of olfactory receptor neurons (ORNs) (Mombaerts, 2004), expression of tdT appeared to be restricted to these primary sensory neurons (Figure 4C). We confirmed this by double-labeling with anti-OMP antibody (164 OMP^+/170 tdT^+ cells, Figure 4D-F). The efficiency of labeling of olfactory neurons following intra-nasal infusion was low, possibly due to interference with viral infection by the mucus layer. In preliminary experiments, we injected H129ΔTK-TT virus into the olfactory bulb of OMP-Cre mice, taking advantage of the ability of H129 virus to infect nerve terminals (Barnett *et al*., 1995; Rinaman and Schwartz, 2004; Song *et al*., 2009). This approach, while more cumbersome technically, appeared to increase the efficiency of infection of ORNs (Supplemental Figure 1R-S).

Transport of H129ΔTK-TT from the MOE to Olfacto-Recipient Nuclei in the Brain

Due to the unpredictable survival times of infected mice, it was difficult to perform a prospective time-course of labeling in the olfactory system as a function of DPI. As an alternative, therefore, animals were retrospectively separated post-mortem into two groups, according to the severity of their symptoms. Infected mice that showed mildly adverse symptoms (slightly hunched back; 6-7 DPI) exhibited spread only to secondary olfactory structures (Suppl. Fig. 5D), while those that showed severe adverse symptoms (hunched back, ungroomed coat, weight loss, nasal and lacrimal excretions; 7-8 DPI) exhibited viral spread in tertiary olfactory structures (Suppl. Fig. 5C), as described below.

ORNs in the MOE synapse in the olfactory bulb with periglomerular interneurons and mitral/tufted relay neurons (reviewed in (Mombaerts *et al*., 1996)). In animals with milder symptoms, tdT expression was observed in the somata (Figure 4G-H, arrows) and dendrites of mitral cells (Figure 4H, arrowhead), as well as occasionally in periglomerular cells (Figure 4I). Among so-called secondary olfactory structures (Haberly, 2001), tdT expression was seen in the dorsal, posterior ventral, lateral, and medial parts of the anterior olfactory nucleus AON (Figure 4J-L), olfactory tubercles (Supplemental Figure 4A-C), piriform cortex (Figure 4M-O), anterior cortical amygdala (Supplemental Figure 4J-L) and entorhinal cortex (Supplemental Figure 4D-F). In animals with more severe symptoms, tdT labeling was observed in tertiary olfactory structures including the insular cortex (Figure 4P-R), orbital frontal cortex (ORB, Supplemental Figure 4G-I), and hippocampus (HPF, Supplemental Figure 4M-O).

Transport of H129ΔTK-TT in the olfactory system is anterograde-specific

To investigate further the anterograde specificity of H129ΔTK-TT, we examined the labeling of several classes of neuromodulatory neurons that project directly to the olfactory bulb. We performed this analysis in OMP-Cre mice that exhibited milder symptoms at 6 to 7 DPI. These mice exhibited tdT expression in the MOE, MOB, piriform cortex (Supplemental Figure 4P-QQ) and olfactory tubercles (data not shown). Despite this multi-synaptic anterograde labeling, we did not detect tdT expression in any of the neuromodulatory populations that project to the MOB, including noradrenergic neurons in the LC (Supplemental Figure 4R-SS, green) (Guevara-aguilar, 1982; Shipley *et al*., 1985), cholinergic neurons in the horizontal limb of the diagonal band (HDB) (Supplemental Figure 4T-UU) (Zaborszky *et al*., 1986), or serotonergic neurons in the raphe nuclei (Supplemental Figure 4V-WW) (McLean and Shipley, 1987). In mice that showed more advanced symptoms and a wider spread of expression (7-8 DPI), tdT was detected in these neuromodulatory populations (Supplemental Table 3c). However this labeling may derive

from higher-order olfactory structures known to project to these neuromodulatory centers, including the insular cortex (Peyron *et al*., 1998), periaqueductal gray (PAG), medial preoptic area (MPO), medial prefontal cortex, central nucleus of the amygdala (CEA), and nucleus tractus solitarius (NTS) (Ennis *et al*., 1998), all of which structures contained tdT^+ cells in these mice (Supplemental Table 3c and Supplemental Fig. 5C).

Transport of H129ΔTK-TT from the VNO to Olfacto-Recipient Nuclei in the Brain

Pheromone-sensing neurons of the vomeronasal organ (VNO) also express OMP, and were labeled in OMP-Cre mice infected intra-nasally with H129ΔTK-TT virus (Fig. 5B, C). The VNO projects to the accessory olfactory bulb (AOB) through the vomeronasal nerves. The AOB in turn projects to a few areas including the medial amygdala (MeA) and the bed nucleus of the stria terminalis (BST) (Scalia and Winans, 1975; Yoon *et al*., 2005), which send further projections to the medial hypothalamic area (Swanson and Petrovich, 1998). We detected tdT expression in the AOB (Figure 5D-F), MeA (Figure 5G-I), BST (Figure 5J-L), and medial preoptic area (MPOA) in the medial hypothalamus (Figure 5M-O), consistent with labeling of the VNO pathway.

In contrast to the relatively limited labeling of brain structures by H129ΔTK-TT in the visual and cerebellar systems, 13.5% (113/836) of anatomically defined brain structures (Franklin and Paxinos, 2008) were labeled by the virus in the olfactory system after 7-8 DPI (Supplemental Table 3c). In general, infected structures, such as the ventromedial hypothalamic nucleus (VMH), which are more synapses removed from the MOE, exhibited a smaller percentage of tdT positive cells than those separated by fewer synapses, such as the AON (Supplemental Figure 5C-D), consistent with the idea that spread is predominantly synaptic.

DISCUSSION

Several viral systems for conditional retrograde trans-synaptic tracing have been developed (reviewed in (Callaway, 2008; Ekstrand *et al*., 2008)), but an analogous system for conditional anterograde trans-synaptic viral tracing *in vivo* has not been implemented. Here we have developed such a method by using homologous recombination (Weir and Dacquel, 1995) to manipulate the genome of the H129 strain of HSV (Dix *et al*., 1983), a well-characterized anterograde trans-synaptic tracer virus (Zemanick *et al*., 1991). Using lines of transgenic mice specifically expressing Cre recombinase, we tested this recombinant virus in the visual, cerebellar and olfactory systems, respectively. In each case, the pattern of labeling obtained was Cre-dependent, concordant with previously described patterns of connectivity, and consistent with an anterograde mode of trans-neuronal transfer.

Synaptic specificity of H129ΔTK-TT labeling

The use of alpha herpesvirus-based transneuronal tracers, such as pseudorabies virus (Ekstrand *et al*., 2008), has been criticized based not only on their toxicity, but on the contention that the virus can spread in a non-synaptic manner to fibers-of-passage or even to glial cells (Ugolini, 2008; Ugolini, 2010). In our studies, the overall pattern of labeling observed in the three systems examined was remarkably specific, and consistent with patterns of connectivity revealed by classical methods. We found little or no evidence of spread to glia (Fig. 2R and Supplemental Figure 2), even in regions where glia were closely juxtaposed with tdT-labeled neurons (e.g., sustentacular cells in the MOE and Muller glia in the retina). While it is difficult to completely exclude non-synaptic spread, little or no labeling of photoreceptors, or of oculomotor neurons in the Edinger-Westphal nuclei, was obtained in our retinal injections. We also failed to detect labeling of neuromodulatory afferents to the olfactory bulb at early time points. All of these data are consistent with the

reported anterograde-specific pattern of labeling by the H129 strain (Rinaman and Schwartz, 2004; Sun et al., 1996; Zemanick et al., 1991). The lack of specificity reported by others for HSV (Ugolini, 2008; Ugolini, 2010) likely reflects the use of different strains of these Herpes viruses.

Synaptic pathways revealed by H129ΔTK-TT

The pattern of labeling obtained in each of the three test systems employed here was complex, as would be expected given the polysynaptic nature of the labeling method. In the visual system, we estimate that at least 4 synapses were crossed by the virus in series (rod BP→AII amacrine→RGC→LGN→V1), with the expected pattern of parallel labeling in subcortical structures such as the superior colliculus and suprachiasmatic nucleus. The pattern obtained is consistent with earlier studies using intra-vitreal injection of native H129 (Sun *et al*., 1996), with the important exception that we observed little or no labeling of photoreceptors, consistent with the Cre-dependence and anterograde specificity of the virus.

In addition to well-characterized sites of visual pathway labeling, we detected the viral reporter in a variety of subcortical sites not previously reported (Sun *et al*., 1996) including, surprisingly, the paraventricular hypothalamic nucleus (PVH) and the ventral lateral septal nucleus (LSV), both of which are involved in stress and anxiety (Sawchenko *et al*., 1996; Sheehan *et al*., 2004). Detection of these sites was facilitated by the very bright native fluorescence of the tdT reporter, and may explain why they were not observed in previous studies using immunohistochemistry to detect H129 antigens (Sun *et al*., 1996). As with any new technique, it is important that unexpected results are verified by independent methods, and therefore these observations should be interpreted with caution. Nevertheless, current evidence suggests that there may be at least 20 different classes of RGCs in the mouse (Badea and Nathans, 2004; Coombs et al., 2006; Sun et al., 2002; Volgyi et al., 2009), many with distinct feature-detector properties (Kim et al., 2008; Lettvin et al., 1959), and at least some of which have distinct patterns of central connectivity (Kay *et al*., 2011). It is therefore tempting to speculate that the labeling of PVN and LSV may reflect specific visual pathways involved in the detection of features associated with threats, such as predators, and wired centrally to evoke alarm or defensive responses (Gollisch and Meister, 2010; Lettvin et al., 1959).

In the olfactory system, the use of traditional neuroanatomical tracers (Buonviso et al., 1991; Haberly and Price, 1977; Luskin and Price, 1982; Ojima et al., 1984; Price, 1973; Scott et al., 1980), as well as the development of novel tracing methods (Ghosh *et al*., 2011; Miyamichi *et al*., 2011; Sosulski *et al*., 2011) have revealed the pattern of projections from the MOE to second- and third-order olfactory structures such as the piriform and accessory olfactory cortices. However, extending such maps beyond these structures has been difficult. Here, infection of primary olfactory sensory neurons in the MOE of OMP-Cre mice with the H129ΔT-TT virus yielded labeling in multiple higher-order structures, including the lateral entorhinal cortex, hippocampus, hypothalamus and, at longer survival times, even midbrain and hindbrain structures (Supplemental Fig. 5 and Table 3c). Remarkably, the percentage of total (836) brain structures labeled from the MOE was 3 fold higher than that labeled in the visual or cerebellar systems (Fig. 6 and Supplemental Tables 3). Quantitative comparisons between different neural systems labeled by this method are difficult, due to potential differences in the efficiency of infection or of trans-synaptic spread. Nevertheless, the engagement of a large fraction of the brain by olfactory afferents is consistent with the widespread ramification of fibers revealed by labeling of individual OB glomeruli with non-transneuronal anterograde tracers (Sosulski *et al*., 2011), and likely reflects the importance of olfaction for both learned and innate behaviors in mice.

One obvious application of this technology is the trans-neuronal labeling of pathways engaged by neurons expressing a specific, behaviorally relevant olfactory receptor, e.g., those involved in pheromone detection (Mombaerts *et al*., 1996). However, the efficiency of labeling in the MOE and VNO was low, presumably due to the inhibition of viral spread by mucus, and in pilot experiments we were unable to detect labeling in mice expressing Cre recombinase under the control of a specific olfactory receptor, MOR28, that is expressed in ~1% of ORNs (Mombaerts, 2006). Nevertheless, our preliminary data suggest that this problem may be overcome by injection of the virus into the olfactory bulb, where infection of ORN axons can occur followed by retrograde transport to the cell body and recombination in ORNs (Supplemental Figure 1R, S).

Limitations

The methodology described here, while powerful, has certain limitations. First, like other replicating trans-neuronal tracers (Callaway, 2008; Ekstrand *et al*., 2008), HSV-based tracers are toxic and kill infected neurons, as well as eventually the whole animal (see Supplemental Table 2). This limits the number of days that an injected animal can be maintained before analysis. Furthermore, there is unpredictable variability in survival times, reflecting variability in the initial level of infection. This makes it currently difficult to perform prospective time-course studies of the progression of labeling in a given pathway, except in a retrospective manner (Supplemental Figure 5C, D). In addition, due to viral cytotoxicity, in animals sacrificed after longer incubation times the initial sites of infection have often been cleared from the brain by macrophages, obscuring the identification of initial relays in a pathway. This limitation may be overcome by analyzing animals exhibiting mild symptoms and/or after shorter survival times, in order to identify the pattern of labeling in early structures.

Second, although virus released endogenously from infected neurons appears to be taken up exclusively by dendrites and transported in the anterograde direction (Zemanick *et al*., 1991), exogenously injected virus can clearly infect nerve terminals and undergo retrograde transport to the cell body, as reported previously (Barnett *et al*., 1995; Rinaman and Schwartz, 2004; Song *et al*., 2009) and confirmed here in the olfactory and cerebellar systems (Supplemental Figure 1P-S). One simple explanation for this paradox is that endogenously produced virus may be released from infected neurons exclusively at pre-synaptic terminals, and therefore uptake is restricted to dendrites of post-synaptic cells, whereas exogenously introduced (injected) virus is accessible to nerve terminals as well as dendrites. Thus, if an injection site of interest (containing Cre-expressing neuronal somata) also contains nerve terminals that coincidentally derive from Cre-expressing neurons located elsewhere in the brain, infection and recombination in such Cre-expressing afferent neurons could occur. Further trans-neuronal spread from such ectopic “starter sites” could render the interpretation of labeling patterns difficult. At present, this confound can be avoided by first injecting the region of interest with a Cre-dependent virus capable of nerve-terminal infection and retrograde transport (e.g., an rAAV of the appropriate serotype), to check whether there are afferents to that region from Cre-expressing neurons elsewhere in the brain.

The ability to engineer the H129 strain by homologous recombination, both in mammalian cells and potentially via recombineering (Smith and Enquist, 2000), opens up the possibility of addressing some of these limitations by further modifications of the viral genome (for genome sequences see (Szpara *et al*., 2010)). This includes introducing modifications designed to mitigate viral toxicity (Lilley *et al*., 2001) and restrict transfer to monosynaptic targets (Wickersham *et al*., 2007). Most importantly, if the problem of neurotoxicity can be solved, it would allow powerful applications of the method to anterograde trans-neuronal delivery not only of marker genes, but of effectors for manipulation of neuronal activity as

well (Luo *et al*., 2008). Such an application would permit a truly systematic functional dissection of specific neural circuits.

EXPERIMENTAL PROCEDURES

Viruses, Plasmids and Generation of H129ΔTK-TT

The H129 strain of HSV-1, a gift from Dr, Lynn W. Enquist, Princeton University), was propagated on Vero cells (ATCC, Manassas, VA) in Eagle's minimal essential medium (EMEM with L-Glutamine) containing 10% fetal bovine serum (FBS) and antibiotics. All viral work was conducted under protocols approved by the Caltech Institute Biological Safety Committee (IBC). To generate the H129ΔTK-TT recombinant virus, a gene targeting construct that contained a *CAG* promoter-driven *loxPSTOPloxP-tdTomato-2A-codon-modified HTK(cmHTK)* cassette, flanked by 5' and 3' homology arms of *HTK* sequences, was co-transfected into HEK293T cells together with native H129 genomic DNA. Recombinant H129 viruses were identified by selection for growth in the presence of acyclovir, which kills cells expressing HTK. Further methodological details are provided in Supplemental Experimental Procedures.

Mice, Viral Injections and Immunohistochemistry

All animal experiments were conducted under protocols approved by the Caltech Institutional Animal Care and Use Committee (IACUC). Two to three-month-old OMP-Cre (gift from Joseph A. Gogos), PCP2/L7-Cre (The Jackson Laboratory, Bar Harbor, ME), or wild-type C57BL/6 (Charles River Laboratory, Wilmington, MA) mice were used. The PCP2/L7-Cre transgenic mice carry a co-integrated *PCP/L7-GFP* transgene. Intranasal injection of H129ΔTK-TT recombinant virus into OMP-Cre mice was performed by slow instillation through one nostril in anaesthetized animals. Intra-ocular (vitreal) injection of virus into anaesthetized PCP2/L7-Cre mice was performed by scleral puncture. Injection of virus into the cerebellum was carried out under deep anaesthesia using a sterotaxic frame. Mice were monitored daily for the development of symptoms: mild symptoms included a slightly hunched back and increased anxiety; more severe symptoms (indicative of more widespread viral infection) included an ungroomed coat, weight loss, and nasal or lacrimal excretions. Mice showing such severe symptoms were immediately euthanized by cardiac perfusion, and brain tissue collected for histological analysis by cryo-sectioning. tdTomato expression was visualized by native fluorescence, while other markers (NeuN, GFAP, etc.) were detected by immunohistochemistry. Further details are provided in Supplemental Experimental Procedures.

Supplementary Material

Refer to Web version on PubMed Central for supplementary material.

Acknowledgments

We thank Dr. L. Enquist for the H129 strain of HSV1, advice and encouragement throughout this project and for feedback on the manuscript, Dr. Jerry Weir for plasmid pGAL10, Dr. Joseph Gogos for OMP-Cre mice, Dr. Markus Meister for help with visual system circuitry, Drs. A. Basbaum and E. Callaway for helpful comments on the manuscript, G. Mosconi and H. Oates-Barker for laboratory management and G. Mancuso for administrative assistance. This work was supported by NIH grant 1RO1MH070053. D.J.A. is an Investigator of the Howard Hughes Medical Institute.

References

Archin NM, van den Boom L, Perelygina L, Hilliard JM, Atherton SS. Delayed spread and reduction in virus titer after anterior chamber inoculation of a recombinant of HSV-1 expressing IL-16. Invest Ophthalmol Vis Sci. 2003; 44:3066–3076. [PubMed: 12824253]

Astic L, Saucier D, Coulon P, Lafay F, Flamand A. The CVS strain of rabies virus as transneuronal tracer in the olfactory system of mice. Brain Res. 1993; 619:146–156. [PubMed: 7690671]

Badea TC, Nathans J. Quantitative analysis of neuronal morphologies in the mouse retina visualized by using a genetically directed reporter. J Comp Neurol. 2004; 480:331–351. [PubMed: 15558785]

Bak IJ, Markham CH, Cook ML, Stevens JG. Intraaxonal transport of Herpes simplex virus in the rat central nervous system. Brain Res. 1977; 136:415–429. [PubMed: 72587]

Barnett EM, Evans GD, Sun N, Perlman S, Cassell MD. Anterograde tracing of trigeminal afferent pathways from the murine tooth pulp to cortex using herpes simplex virus type 1. J Neurosci. 1995; 15:2972–2984. [PubMed: 7536824]

Barski JJ, Dethleffsen K, Meyer M. Cre recombinase expression in cerebellar Purkinje cells. Genesis. 2000; 28:93–98. [PubMed: 11105049]

Beier KT, Saunders A, Oldenburg IA, Miyamichi K, Akhtar N, Luo L, Whelan SP, Sabatini B, Cepko CL. Anterograde or retrograde transsynaptic labeling of CNS neurons with vesicular stomatitis virus vectors. Proc Natl Acad Sci U S A. 2011; 108:15414–15419. [PubMed: 21825165]

Bock DD, Lee WC, Kerlin AM, Andermann ML, Hood G, Wetzel AW, Yurgenson S, Soucy ER, Kim HS, Reid RC. Network anatomy and in vivo physiology of visual cortical neurons. Nature. 2011; 471:177–182. [PubMed: 21390124]

Bohland JW, Wu C, Barbas H, Bokil H, Bota M, Breiter HC, Cline HT, Doyle JC, Freed PJ, Greenspan RJ, et al. A proposal for a coordinated effort for the determination of brainwide neuroanatomical connectivity in model organisms at a mesoscopic scale. PLoS Comput Biol. 2009; 5:e1000334. [PubMed: 19325892]

Branda CS, Dymecki SM. Talking about a revolution: The impact of site-specific recombinases on genetic analyses in mice. Dev Cell. 2004; 6:7–28. [PubMed: 14723844]

Braz JM, Rico B, Basbaum AI. Transneuronal tracing of diverse CNS circuits by Cre-mediated induction of wheat germ agglutinin in transgenic mice. Proc Natl Acad Sci U S A. 2002; 99:15148–15153. [PubMed: 12391304]

Briggman KL, Helmstaedter M, Denk W. Wiring specificity in the direction-selectivity circuit of the retina. Nature. 2011; 471:183–188. [PubMed: 21390125]

Brumberg JC, Hamzei-Sichani F, Yuste R. Morphological and physiological characterization of layer VI corticofugal neurons of mouse primary visual cortex. J Neurophysiol. 2003; 89:2854–2867. [PubMed: 12740416]

Buonviso N, Revial MF, Jourdan F. The Projections of Mitral Cells from Small Local Regions of the Olfactory Bulb: An Anterograde Tracing Study Using PHA-L (Phaseolus vulgaris Leucoagglutinin). Eur J Neurosci. 1991; 3:493–500. [PubMed: 12106481]

Callaway EM. Transneuronal circuit tracing with neurotropic viruses. Current Opinion in Neurobiology. 2008; 18:617–623. [PubMed: 19349161]

Card JP, Enquist LW. Transneuronal circuit analysis with pseudorabies viruses. Current Protocols in Neuroscience. 1999:1.5.1–1.5.28.

Card JP, Kobiler O, Ludmir EB, Desai V, Sved AF, Enquist LW. A dual infection pseudorabies virus conditional reporter approach to identify projections to collateralized neurons in complex neural circuits. PLoS One. 2011a; 6:e21141. [PubMed: 21698154]

Card JP, Kobiler O, McCambridge J, Ebdlahad S, Shan Z, Raizada MK, Sved AF, Enquist LW. Microdissection of neural networks by conditional reporter expression from a Brainbow herpesvirus. Proc Natl Acad Sci U S A. 2011b; 108:3377–3382. [PubMed: 21292985]

Coombs J, van der List D, Wang GY, Chalupa LM. Morphological properties of mouse retinal ganglion cells. Neuroscience. 2006; 140:123–136. [PubMed: 16626866]

Danciger E, Mettling C, Vidal M, Morris R, Margolis F. Olfactory marker protein gene: its structure and olfactory neuron-specific expression in transgenic mice. Proc Natl Acad Sci U S A. 1989; 86:8565–8569. [PubMed: 2701951]

DeFalco J, Tomishima M, Liu H, Zhao C, Cai X, Marth JD, Enquist L, Friedman JM. Virus-assisted mapping of neural inputs to a feeding center in the hypothalamus. Science. 2001; 291:2608–2613. [PubMed: 11283374]

Dix RD, McKendall RR, Baringer JR. Comparative neurovirulence of herpes simplex virus type 1 strains after peripheral or intracerebral inoculation of BALB/c mice. Infect Immun. 1983; 40:103–112. [PubMed: 6299955]

Dong, HW. The Allen references atlas: A digital color brain atlas of the C57Bl/6J male mouse. Hoboken, N.J.: John Wiley & Sons, Inc.; 2008.

Drager UC. Autoradiography of tritiated proline and fucose transported transneuronally from the eye to the visual cortex in pigmented and albino mice. Brain Res. 1974; 82:284–292. [PubMed: 4441894]

Dum RP, Levinthal DJ, Strick PL. The Spinothalamic System Targets Motor and Sensory Areas in the Cerebral Cortex of Monkeys. Journal of Neuroscience. 2009; 29:14223–14235. [PubMed: 19906970]

Dymecki SM, Ray RS, Kim JC. Mapping cell fate and function using recombinase-based intersectional strategies. Methods Enzymol. 2010; 477:183–213. [PubMed: 20699143]

Eggan K, Baldwin K, Tackett M, Osborne J, Gogos J, Chess A, Axel R, Jaenisch R. Mice cloned from olfactory sensory neurons. Nature. 2004; 428:44–49. [PubMed: 14990966]

Ekstrand MI, Enquist LW, Pomeranz LE. The alpha-herpesviruses: molecular pathfinders in nervous system circuits. Trends Mol Med. 2008; 14:134–140. [PubMed: 18280208]

Ennis M, Shipley MT, Aston-Jones G, Williams JT. Afferent control of nucleus locus ceruleus: differential regulation by “shell” and “core” inputs. Adv Pharmacol. 1998; 42:767–771. [PubMed: 9328011]

Franklin, KBJ.; Paxinos, G. The Mouse Brain in Stereotaxic Coordinates. New York: Academic Press; 2008.

Frost DO, Caviness VS Jr. Radial organization of thalamic projections to the neocortex in the mouse. J Comp Neurol. 1980; 194:369–393. [PubMed: 7440806]

Ghosh S, Larson SD, Hefzi H, Marnoy Z, Cutforth T, Dokka K, Baldwin KK. Sensory maps in the olfactory cortex defined by long-range viral tracing of single neurons. Nature. 2011; 472:217–220. [PubMed: 21451523]

Gollisch T, Meister M. Eye smarter than scientists believed: neural computations in circuits of the retina. Neuron. 2010; 65:150–164. [PubMed: 20152123]

Guevara-aguilar R. Differential projections from locus coeruleus to olfactory bulb and olfactory tubercle: an HRP study. Brain Reseach Bulletin. 1982; 8:711–719.

Haberly LB. Parallel-distributed processing in olfactory cortex: new insights from morphological and physiological analysis of neuronal circuitry. Chem Senses. 2001; 26:551–576. [PubMed: 11418502]

Haberly LB, Price JL. The axonal projection patterns of the mitral and tufted cells of the olfactory bulb in the rat. Brain Res. 1977; 129:152–157. [PubMed: 68803]

Hattar S, Kumar M, Park A, Tong P, Tung J, Yau K-W, Berson DM. Central projections of melanopsin-expressing retinal ganglion cells in the mouse. The journal of comparative neurology. 2006; 497:326–349. [PubMed: 16736474]

Haubensak W, Kunwar PS, Cai H, Ciocchi S, Wall NR, Ponnusamy R, Biag J, Dong HW, Deisseroth K, Callaway EM, et al. Genetic dissection of an amygdala microcircuit that gates conditioned fear. Nature. 2010; 468:270–276. [PubMed: 21068836]

Haverkamp S. Immunocytochemical Analysis of the Mouse Retina. The journal of comparative neurology. 2000; 424:1–23. [PubMed: 10888735]

Hoffer BJ, Siggins GR, Oliver AP, Bloom FE. Activation of the pathway from locus coeruleus to rat cerebellar Purkinje neurons: pharmacological evidence of noradrenergic central inhibition. J Pharmacol Exp Ther. 1973; 184:553–569. [PubMed: 4347049]

Horowitz LF, Montmayeur JP, Echelard Y, Buck LB. A genetic approach to trace neural circuits. Proc Natl Acad Sci U S A. 1999; 96:3194–3199. [PubMed: 10077660]

Ito, M. The cerebellum and neural control. New York: Raven Press; 1984.

Jurrus E, Hardy M, Tasdizen T, Fletcher PT, Koshevoy P, Chien CB, Denk W, Whitaker R. Axon tracking in serial block-face scanning electron microscopy. Med Image Anal. 2009; 13:180–188. [PubMed: 18617436]

Katz LC, Burkhalter A, Dreyer WJ. Fluorescent latex microspheres as a retrograde neuronal marker for in vivo and in vitro studies of visual cortex. Nature. 1984; 310:498–500. [PubMed: 6205278]

Kay JN, De la Huerta I, Kim IJ, Zhang Y, Yamagata M, Chu MW, Meister M, Sanes JR. Retinal ganglion cells with distinct directional preferences differ in molecular identity, structure, and central projections. J Neurosci. 2011; 31:7753–7762. [PubMed: 21613488]

Kelly RM, Strick PL. Cerebellar loops with motor cortex and prefrontal cortex of a nonhuman primate. J Neurosci. 2003; 23:8432–8444. [PubMed: 12968006]

Kim IJ, Zhang Y, Yamagata M, Meister M, Sanes JR. Molecular identification of a retinal cell type that responds to upward motion. Nature. 2008; 452:478–482. [PubMed: 18368118]

Kissa K, Mordelet E, Soudais C, Kremer EJ, Demeneix BA, Brulet P, Coen L. In vivo neuronal tracing with GFP-TTC gene delivery. Mol Cell Neurosci. 2002; 20:627–637. [PubMed: 12213444]

Kleinfeld D, Bharioke A, Blinder P, Bock DD, Briggman KL, Chklovskii DB, Denk W, Helmstaedter M, Kaufhold JP, Lee WC, et al. Large-Scale Automated Histology in the Pursuit of Connectomes. J Neurosci. 2011; 31:16125–16138. [PubMed: 22072665]

Kobbert C, Apps R, Bechmann I, Lanciego JL, Mey J, Thanos S. Current concepts in neuroanatomical tracing. Prog Neurobiol. 2000; 62:327–351. [PubMed: 10856608]

Kolb H. Amacrine Cells of the Cat Retina. Vision Res. 1981; 21:1625–1633. [PubMed: 7336596]

Kozloski J, Hamzei-Sichani F, Yuste R. Stereotyped position of local synaptic targets in neocortex. Science. 2001; 293:868–872. [PubMed: 11486089]

Lettvin JY, Maturana HR, McCulloch WS, Pitts WH. What the frog's eye tells the frog's brain. Proceedings of the Institute of Radio Engineers. 1959; 47:1940–1951.

Lilley CE, Groutsi F, Han Z, Palmer JA, Anderson PN, Latchman DS, Coffin RS. Multiple immediate-early gene-deficient herpes simplex virus vectors allowing efficient gene delivery to neurons in culture and widespread gene delivery to the central nervous system in vivo. J Virol. 2001; 75:4343–4356. [PubMed: 11287583]

Lundh B. Spread of vesicular stomatitis virus along the visual pathways after retinal infection in the mouse. Acta Neuropathol. 1990; 79:395–401. [PubMed: 2160183]

Luo L, Callaway EM, Svoboda K. Genetic dissection of neural circuits. Neuron. 2008; 57:634–660. [PubMed: 18341986]

Luskin MB, Price JL. The distribution of axon collaterals from the olfactory bulb and the nucleus of the horizontal limb of the diagonal band to the olfactory cortex, demonstrated by double retrograde labeling techniques. J Comp Neurol. 1982; 209:249–263. [PubMed: 7130455]

Martin X, Dolivo M. Neuronal and transneuronal tracing in the trigeminal system of the rat using the herpes virus suis. Brain Res. 1983; 273:253–276. [PubMed: 6311350]

McLean JH, Shipley MT. Serotonergic afferents to the rat olfactory bulb: I. Origins and laminar specificity of serotonergic inputs in the adult rat. J Neurosci. 1987; 7:3016–3028. [PubMed: 2822862]

Millhouse O. Optic chiasmcollaterals afferent to the suprachiasmatic nucleus. Brain Res. 1977; 137:351–355. [PubMed: 589458]

Miyamichi K, Amat F, Moussavi F, Wang C, Wickersham I, Wall NR, Taniguchi H, Tasic B, Huang ZJ, He Z, et al. Cortical representations of olfactory input by trans-synaptic tracing. Nature. 2011; 472:191–196. [PubMed: 21179085]

Mombaerts P. Genes and ligands for odorant, vomeronasal and taste receptors. Nat Rev Neurosci. 2004; 5:263–278. [PubMed: 15034552]

Mombaerts P. Axonal wiring in the mouse olfactory system. Annu Rev Cell Dev Biol. 2006; 22:713–737. [PubMed: 17029582]

Mombaerts P, Wang F, Dulac C, Vassar R, Chao SK, Nemes A, Mendelsohn M, Edmondson J, Axel R. The molecular biology of olfactory perception. Cold Spring Harb Symp Quant Biol. 1996; 61:135–145. [PubMed: 9246442]

Norgren RB Jr, Lehman MN. Herpes simplex virus as a transneuronal tracer. Neurosci Biobehav Rev. 1998; 22:695–708. [PubMed: 9809305]

Oberdick J, Smeyne RJ, Mann JR, Zackson S, Morgan JI. A promoter that drives transgene expression in cerebellar Purkinje and retinal bipolar neurons. Science. 1990; 248:223–226. [PubMed: 2109351]

Ojima H, Mori K, Kishi K. The trajectory of mitral cell axons in the rabbit olfactory cortex revealed by intracellular HRP injection. J Comp Neurol. 1984; 230:77–87. [PubMed: 6096415]

Pak MW, Giolli RA, Pinto LH, Mangini NJ, Gregory KM, Vanable JW Jr. Retinopretectal and accessory optic projections of normal mice and the OKN-defective mutant mice beige, beige-J, and pearl. J Comp Neurol. 1987; 258:435–446. [PubMed: 3584547]

Peters, A. The visual cortex of the rat. In: Peters, A.; Jones, EG., editors. Cerebral Cortex. New York: Plenum Press; 1985. p. 19-80.

Peyron C, Petit JM, Rampon C, Jouvet M, Luppi PH. Forebrain afferents to the rat dorsal raphe nucleus demonstrated by retrograde and anterograde tracing methods. Neuroscience. 1998; 82:443–468. [PubMed: 9466453]

Price JL. An autoradiographic study of complementary laminar patterns of termination of afferent fibers to the olfactory cortex. J Comp Neurol. 1973; 150:87–108. [PubMed: 4722147]

Provencio I, Cooper HM, Foster RG. Retinal projections in mice with inherited retinal degeneration: implications for circadian photoentrainment. J Comp Neurol. 1998; 395:417–439. [PubMed: 9619497]

Rinaman L, Schwartz G. Anterograde transneuronal viral tracing of central viscerosensory pathways in rats. J Neurosci. 2004; 24:2782–2786. [PubMed: 15028771]

Ross CA, Ruggiero DA, Reis DJ. Afferent projections to cardiovascular portions of the nucleus of the tractus solitarius in the rat. Brain Res. 1981; 223:402–408. [PubMed: 6169408]

Sawchenko PE, Brown ER, Chan RK, Ericsson A, Li HY, Roland BL, Kovacs KJ. The paraventricular nucleus of the hypothalamus and the functional neuroanatomy of visceromotor responses to stress. Prog Brain Res. 1996; 107:201–222. [PubMed: 8782521]

Scalia F, Winans SS. The differential projections of the olfactory bulb and accessory olfactory bulb in mammals. J Comp Neurol. 1975; 161:31–55. [PubMed: 1133226]

Scott JW, McBride RL, Schneider SP. The organization of projections from the olfactory bulb to the piriform cortex and olfactory tubercle in the rat. J Comp Neurol. 1980; 194:519–534. [PubMed: 7451680]

Seung HS. Reading the book of memory: sparse sampling versus dense mapping of connectomes. Neuron. 2009; 62:17–29. [PubMed: 19376064]

Sheehan TP, Chambers RA, Russell DS. Regulation of affect by the lateral septum: implications for neuropsychiatry. Brain Res Brain Res Rev. 2004; 46:71–117. [PubMed: 15297155]

Shipley MT, Halloran FJ, de la Torre J. Surprisingly rich projection from locus coeruleus to the olfactory bulb in the rat. Brain Res. 1985; 329:294–299. [PubMed: 3978450]

Simmons PA, Lemmon V, Pearlman AL. Afferent and efferent connections of the striate and extrastriate visual cortex of the normal and reeler mouse. J Comp Neurol. 1982; 211:295–308. [PubMed: 7174895]

Smith GA, Enquist LW. A self-recombining bacterial artificial chromosome and its application for analysis of herpesvirus pathogenesis. Proc Natl Acad Sci USA. 2000; 97:4873–4878. [PubMed: 10781094]

Snider RS, Maiti A, Snider SR. Cerebellar pathways to ventral midbrain and nigra. Exp Neurol. 1976; 53:714–728. [PubMed: 1001395]

Song C, Enquist L, Bartness T. New developments in tracing neural circuits with herpesviruses. Virus Research. 2005; 111:235–249. [PubMed: 15893400]

Song CK, Schwartz GJ, Bartness TJ. Anterograde transneuronal viral tract tracing reveals central sensory circuits from white adipose tissue. Am J Physiol Regul Integr Comp Physiol. 2009; 296:R501–511. [PubMed: 19109367]

Sosulski DL, Bloom ML, Cutforth T, Axel R, Datta SR. Distinct representations of olfactory information in different cortical centres. Nature. 2011; 472:213–216. [PubMed: 21451525]

Sun N, Cassell MD, Perlman S. Anterograde, transneuronal transport of herpes simplex virus type 1 strain H129 in the murine visual system. J Virol. 1996; 70:5405–5413. [PubMed: 8764051]

Sun W, Li N, He S. Large-scale morphological survey of mouse retinal ganglion cells. J Comp Neurol. 2002; 451:115–126. [PubMed: 12209831]

Swanson LW. Cerebral hemisphere regulation of motivated behavior. Brain research. 2000; 886:113–164. [PubMed: 11119693]

Swanson LW, Petrovich GD. What is the amygdala? Trends Neurosci. 1998; 21:323–331. [PubMed: 9720596]

Szpara ML, Parsons L, Enquist LW. Sequence variability in clinical and laboratory isolates of herpes simplex virus 1 reveals new mutations. J Virol. 2010; 84:5303–5313. [PubMed: 20219902]

Ugolini G. Use of rabies virus as a transneuronal tracer of neuronal connections: implications for the understanding of rabies pathogenesis. Dev Biol (Basel). 2008; 131:493–506. [PubMed: 18634512]

Ugolini G. Advances in viral transneuronal tracing. Journal of Neuroscience Methods. 2010; 194:2–20. [PubMed: 20004688]

Vercelli A, Repici M, Garbossa D, Grimaldi A. Recent techniques for tracing pathways in the central nervous system of developing and adult mammals. Brain Res Bull. 2000; 51:11–28. [PubMed: 10654576]

Volgyi B, Chheda S, Bloomfield SA. Tracer coupling patterns of the ganglion cell subtypes in the mouse retina. J Comp Neurol. 2009; 512:664–687. [PubMed: 19051243]

Wall NR, Wickersham IR, Cetin A, De La Parra M, Callaway EM. Monosynaptic circuit tracing in vivo through Cre-dependent targeting and complementation of modified rabies virus. Proc Natl Acad Sci U S A. 2010; 107:21848–21853. [PubMed: 21115815]

Ward S, Thomson N, White JG, Brenner S. Electron microscopical reconstruction of the anterior sensory anatomy of the nematode Caenorhabditis elegans. J Comp Neurol. 1975; 160:313–337. [PubMed: 1112927]

Wassle H. Parallel processing in the mammalian retina. Nat Rev Neurosci. 2004; 5:747–757. [PubMed: 15378035]

Weible AP, Schwarcz L, Wickersham IR, Deblander L, Wu H, Callaway EM, Seung HS, Kentros CG. Transgenic targeting of recombinant rabies virus reveals monosynaptic connectivity of specific neurons. J Neurosci. 2010; 30:16509–16513. [PubMed: 21147990]

Weir JP, Dacquel EJ. Plasmid insertion vectors that facilitate construction of herpes simplex virus gene delivery vectors. Gene. 1995; 154:123–128. [PubMed: 7867939]

Wickersham IR, Lyon DC, Barnard RJ, Mori T, Finke S, Conzelmann KK, Young JA, Callaway EM. Monosynaptic restriction of transsynaptic tracing from single, genetically targeted neurons. Neuron. 2007; 53:639–647. [PubMed: 17329205]

Yamashita M, Wassle H. Responses of rod bipolar cells isolated from the rat retina to the glutamate agonist 2-Amino-4-phosphonobutyric Acid (APB). The Journal of Neuroscience. 1991; 11:2372–2382. [PubMed: 1714492]

Yoon H, Enquist LW, Dulac C. Olfactory inputs to hypothalamic neurons controlling reproduction and fertility. Cell. 2005; 123:669–682. [PubMed: 16290037]

Yoshihara Y. Visualizing selective neural pathways with WGA transgene: combination of neuroanatomy with gene technology. Neurosci Res. 2002; 44:133–140. [PubMed: 12354628]

Yoshihara Y, Mizuno T, Nakahira M, Kawasaki M, Watanabe Y, Kagamiyama H, Jishage K, Ueda O, Suzuki H, Tabuchi K, et al. A genetic approach to visualization of multisynaptic neural pathways using plant lectin transgene. Neuron. 1999; 22:33–41. [PubMed: 10027287]

Zaborszky L, Carlsen J, Brashear HR, Heimer L. Cholinergic and GABAergic afferents to the olfactory bulb in the rat with special emphasis on the projection neurons in the nucleus of the horizontal limb of the diagonal band. J Comp Neurol. 1986; 243:488–509. [PubMed: 3512629]

Zemanick MC, Strick PL, Dix RD. Direction of transneuronal transport of herpes simplex virus 1 in the primate motor system is strain-dependent. Proc Natl Acad Sci U S A. 1991; 88:8048–8051. [PubMed: 1654557]

Zhang XM, Chen BY, Ng AH, Tanner JA, Tay D, So KF, Rachel RA, Copeland NG, Jenkins NA, Huang JD. Transgenic mice expressing Cre-recombinase specifically in retinal rod bipolar neurons. Invest Ophthalmol Vis Sci. 2005; 46:3515–3520. [PubMed: 16186328]

Zhang XM, Ng AH, Tanner JA, Wu WT, Copeland NG, Jenkins NA, Huang JD. Highly restricted expression of Cre recombinase in cerebellar Purkinje cells. Genesis. 2004; 40:45–51. [PubMed: 15354293]

Zinyk DL, Mercer EH, Harris E, Anderson DJ, Joyner AL. Fate mapping of the mouse midbrain-hindbrain constriction using a site-specific recombination system. Curr Biol. 1998; 8:665–668. [PubMed: 9635195]

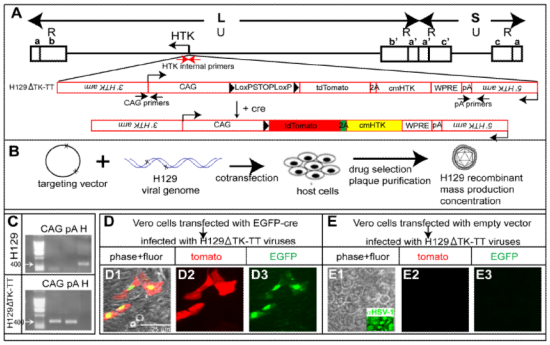

Figure 1. Construction and expression properties of HSV-1 strain H129ΔTK-TT

(A) H129 targeting strategy. Upper, schematic of H129 genome. L, S indicate long and short fragments, respectively; U and R, unique and inverted (a, b, c, and a', b' and c') repeats, respectively. Lower, targeting construct (red). (B) Strategy for generating recombinant H129. (C) Genomic PCR analysis of H129 and H129ΔTK-TT. CAG and pA indicate 3' and 5' junction fragments (see (A)). "H" indicates native HTK fragment (see red arrows in A). (D-E) Infection of Vero cells by H129ΔTK-TT with (D) or without (E) EGFP-Cre transfection. Related data regarding the infectivity of H129ΔTK-TT virus is shown in Supplemental Table 2.

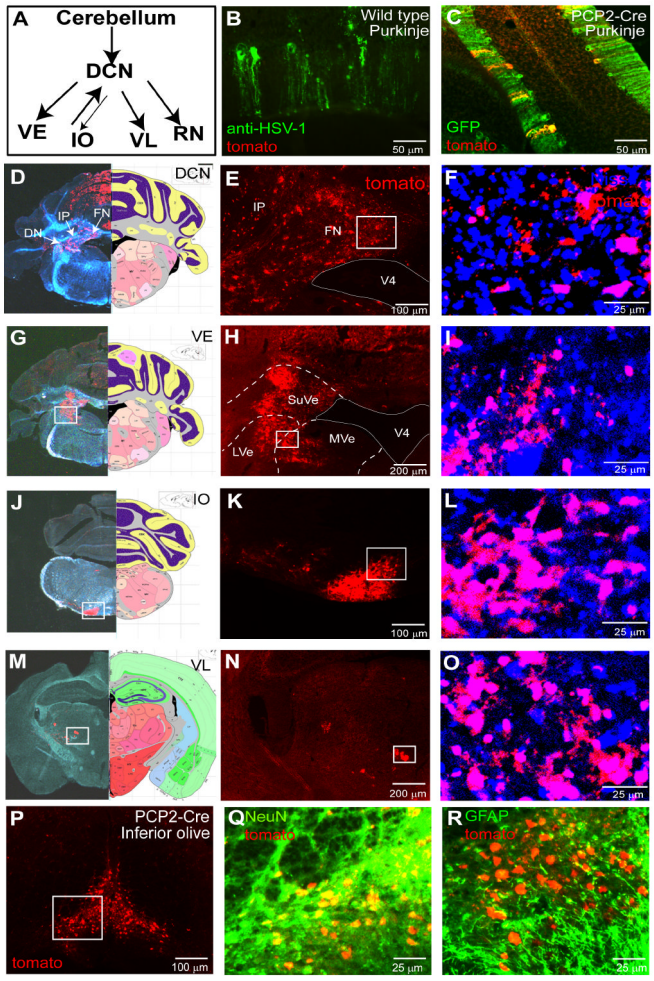

Figure 2. H129ΔTK-TT tracing of cerebellar circuits from Purkinje cells

(A) Schematic illustrating the cerebellar-Purkinje pathway. Two-way arrows indicate the olivo-cerebellar tract and cerebello-olivary pathway (Ito, 1984). DCN, deep cerebellar nucleus; VE, vestibular nucleus; RN, red nucleus; IO, inferior olive; VL, ventral lateral thalamic nucleus. (B-C) Intracerebellar injection of wild type (B) or PCP2/L7-Cre transgenic mice (C) with H129ΔTK-TT virus. GFP (C) reports a co-integrated PCP2/L7-EGFP transgene. (D-O) Brain structures labeled with H129ΔTK-TT following recombination in Purkinje cells. DN, dentate nucleus; IP, interposed nucleus; FN, fastigial nucleus; LVe, lateral vestibular nucleus; MVe, medial vestibular nucleus; SuVe, superior vestibular nucleus; V4, 4th ventricle. Left panels in (D, G, J, M) are from injected brains stained for Nissl and native tdT (merged brightfield/fluorescence); right panels are corresponding sections from Allen Reference Atlas (Dong, 2008). Panels (F, I, L, O) are higher magnification images of boxed regions in (E, H, K, N), respectively, from the same or adjacent sections, counter-stained with fluorescent Nissl. Additional labeled areas are shown in Supplemental Figure 1. (P-R) tdTomato labeling is restricted to neurons in the IO. (Q, R), double-labeling for tdT and anti-NeuN (Q) or GFAP (R) antibody staining, in adjacent sections corresponding to the boxed region in (P). Additional data are shown in Supplemental Figure 2 and Supplemental Table 1.

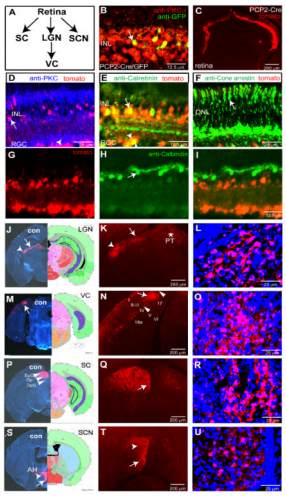

Figure 3. H129ΔTK-TT tracing of visual system circuits from rod bipolar cells

(A) Schematic illustrating visual pathway. (B-I) Retinal sections from PCP2/L7-Cre/GFP mice. (B) GFP and PKCα mark rod bipolar cells (RBCs; arrow) in uninjected mice. (C) Retinal tdT expression following intra-vitreal injection of H129ΔTK-TT virus. (D-I) Note tdT labeling in RBCs (D, arrow), amacrine (E, arrow), and retinal ganglion cells (D, E arrowheads), but not in photoreceptors (F, arrow) or horizontal cells (G-I, arrow). (J-U) Central visual relays labeled by H129ΔTK-TT transport. Left panels in (J, M, P, S) illustrate hemibrains contralateral to injected eye, stained for Nissl and tdT. LGN, lateral geniculate nucleus; PT, pretectal nucleus; VC, visual cortex; (I-VI), layers of visual cortex (N); SC, superior collicullus; SuG, superficial gray of SC; Op, optic nerve layer of SC; DpG; deep gray layer of SC. (S) SCN, suprachiasmatic nucleus; AH, anterior hypothalamus (arrowhead and arrow, respectively, in (T)). (L, O, R, U) are higher magnification views of the labeled areas indicated by arrows in (K, N, Q, T), respectively, counter-stained with fluorescent Nissl. Additional tdT-expressing regions in these mice are shown in Supplemental Figure 3.

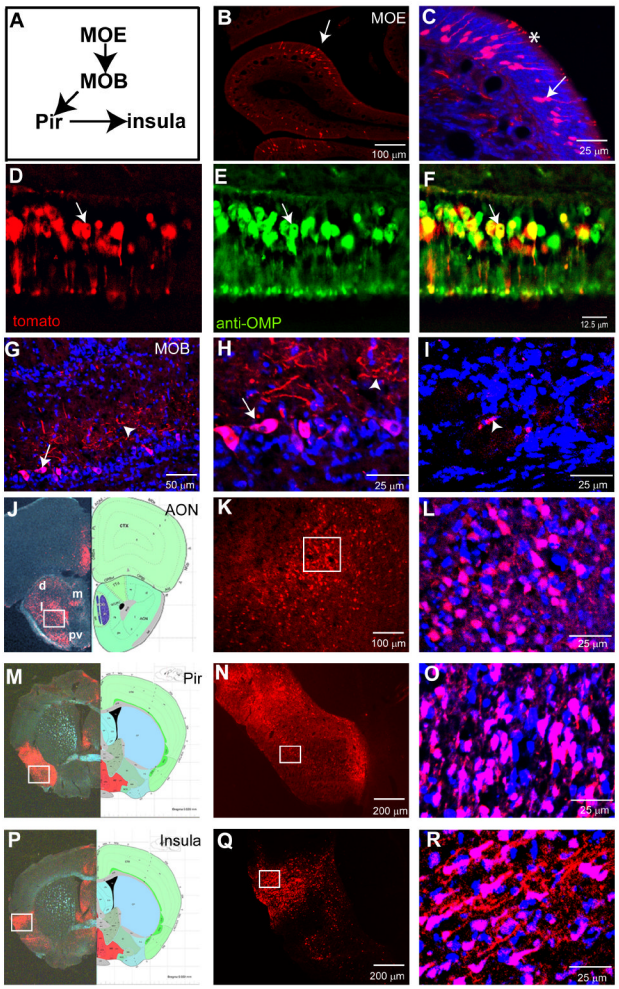

Figure 4. H129ΔTK-TT tracing of main olfactory circuits from ORNs

(A) Schematic illustrating main olfactory pathway. MOE, Main Olfactory Epithelium; MOB, Main Olfactory Bulb; Pir, piriform cortex. (B-F) H129ΔTK-TT infected MOE. Arrows (B-C) indicate labeled ORNs, asterisk olfactory cilia. (D-F) section of MOE double-labeled for tdT and anti-OMP; arrows indicate double-positive ORN. (G-I) Labeling in the MOB. (H) higher magnification view of area indicated by arrow in (G). Arrows indicate mitral cells, arrowheads external plexiform layer in (G, H). Arrowhead in (I) indicates periglomerular cell. (J-R) tdT labeling of higher order main olfactory relays. AON, anterior olfactory nucleus (d, m, l, and pv in (J) indicate dorsal, medial, lateral, and posteroventral parts of AON); Pir, piriform cortex; Insula, insular cortex. Organization of panels as in Figure 2D-O. Additional labeled brain areas are shown in Supplemental Figure 4.

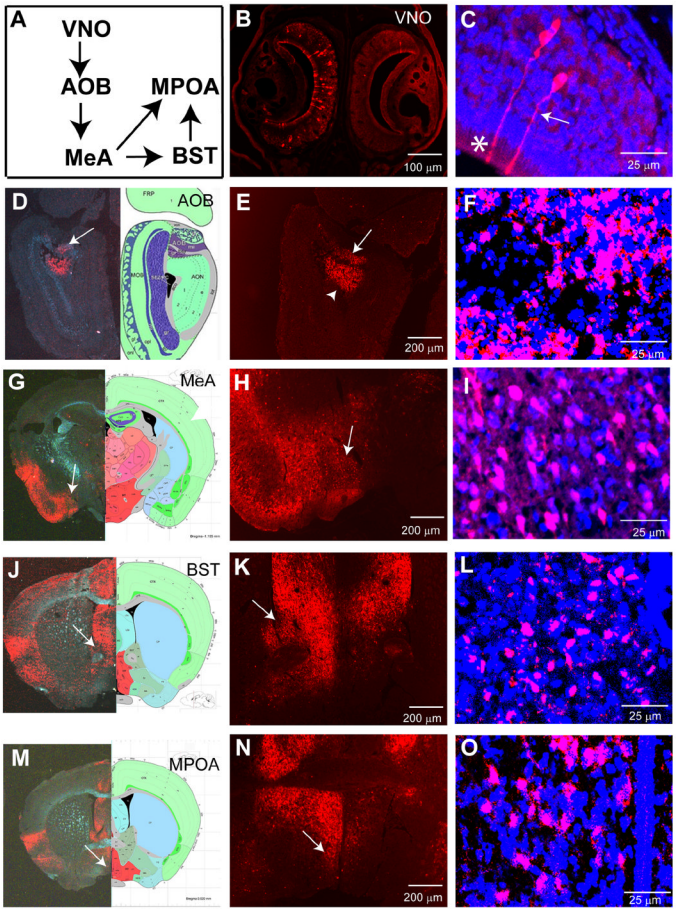

Figure 5. H129ΔTK-TT tracing of accessory olfactory circuits

(A) Schematic illustrating VNO system. AOB, accessory olfactory bulb; MeA, medial amygdala; MPOA, medial preoptic area; BST, bed nucleus of the stria terminalis. (B-C) H129ΔTK-TT infected VNO. Arrow (C) indicates labeled olfactory receptor neuron, asterisk olfactory microvilli. (D-O) tdT labeling of higher order accessory olfactory relays. Arrowhead (E) indicates anterior olfactory nuclei. Organization of panels (D-O) as in Fig. 3(J-U).

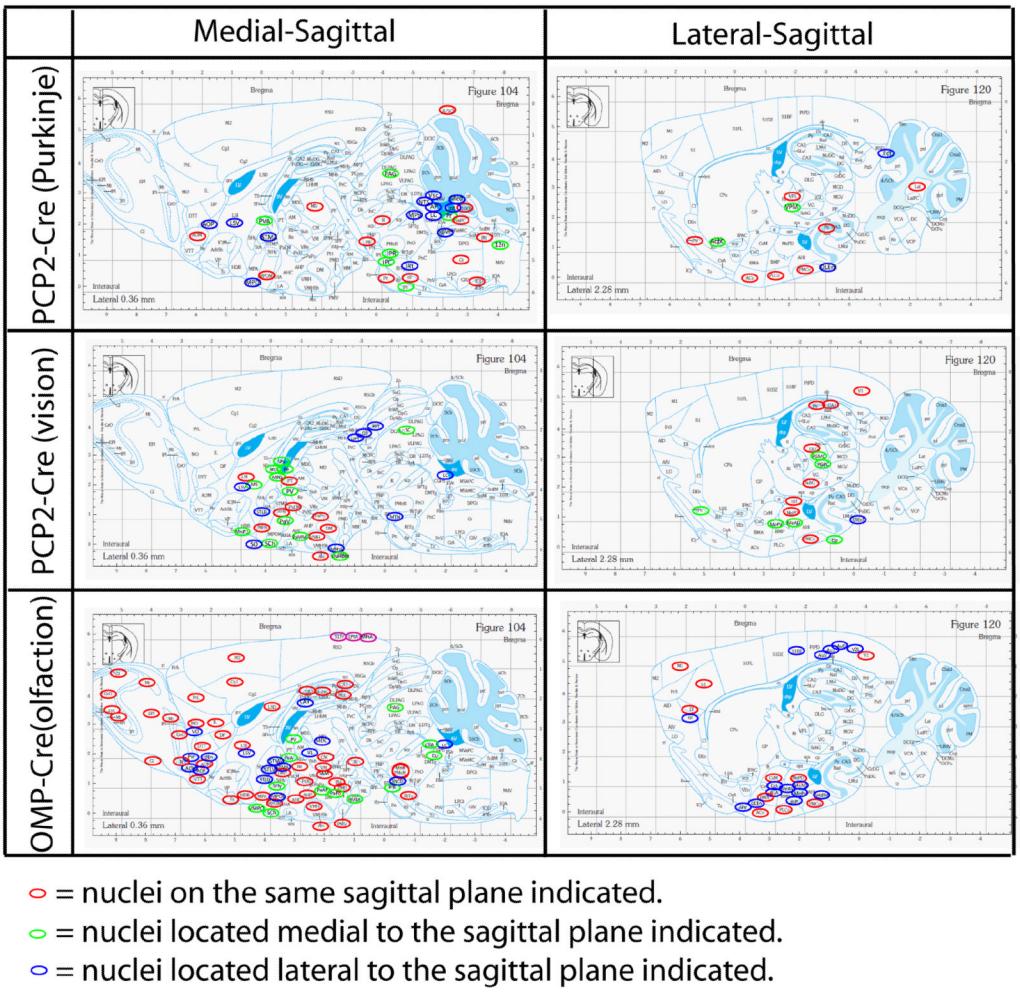

Figure 6. Comparisons of selected brain structures labeled by H129ΔTK-TT in the visual, olfactory, and cerebellar pathways

Medial-sagittal and lateral-sagittal plates and labeled structures are from the Franklin and Paxinos Atlas (Franklin and Paxinos, 2008). Red circles mark tdT-labeled structures on the indicated saggital planes; green and blue circles mark tdT-labeled structures on adjacent medial and lateral planes, respectively. Related data are shown in Supplemental Figure 5 and Supplemental Table 3.